Characterization of porous silicon based optical sensor system for biosensor applications

A. Kovacs, P. Jonnalagadda, X. Y. Meng and U. Mescheder
Institute for Applied Research
Hochschule Furtwangen University
Robert-Gerwig-Platz 1, 78120 Furtwangen, Germany
e-mail: kovacs@hs-furtwangen.de

***Abstract*—Porous silicon based multilayer structures for optical sensors have been simulated, fabricated and tested. The properties of optical sensors using porous silicon multilayer can be adjusted by appropriate substrate material, morphology, process parameters in the pore formation process and by surface treatment (thermal oxidation). Heavily and lightly doped p-doped substrates have been used to realize porous silicon layers with different morphology, porosity (30-80%), pore size (mesoporous range) and specific surface area (200-700m²/cm³). Thermal oxidation stabilizes the surface and results in hydrophilic surfaces for effective adsorption of liquid analytes. Oxidation reduces the porosity and the pore size but improves the wetting behavior of liquid analytes in the porous volume. Different multilayer structures using native and oxidized porous silicon and corresponding concepts of optical sensor systems have been proved for aqueous and organic analytes. Sensors using small pore size (2-4nm) and high porosity (70-80%) have been realized and characterized. A simple, low cost optical sensor system based on multilayer, a tunable light source and a detector has been realized.**

I. INTRODUCTION

Porous silicon (PS) exhibits a great potential in optical sensor applications due to the possibility to tune its refractive index and to use it for detection of biological substances [1-6] or chemical vapor [7]. Especially, multilayer structures with tunable spectral characteristics such as distributed Bragg reflectors (DBR) [8,16], rugate filters [7,9,10,11,15,22] with broadband [12] or narrow line-width [13] and Fabry-Perot filters have been realized [5,8,14,15,17,19,23,24]. The specific spectral properties play an important role for the chosen sensor design and can be tuned by the fabrication parameters, especially the applied current density in the electrochemical etching process.

The material properties such as porosity, pore size distribution and specific surface area depend strongly on the substrate doping [18,19]. Typically high doped p-substrates have been used for the fabrication of porous silicon multilayers (PSMLs) [5,8,10,12,13,17,19,21-24] because of the possibility to get a larger change of refractive index of PS by changing the process conditions. PSMLs fabricated using lightly doped p-substrates exhibit high porosity (70-80%), small pore size (2-5nm) and high specific surface area (in the range of 700m²/cm³) and therefore can be applied successfully especially for chemical vapor detection of organic solvents [7,11,19,22].

Additionally, the sensitivity of an optical sensor depends on the adsorption properties of the measured substances [7,8,20] and the interaction of the specific analyte with the porous silicon matrix, which can be adjusted and improved by proper fabrication parameters. Native porous silicon layers show aging effects, therefore, a subsequent process has to be considered to stabilize the internal surfaces in the porous material. Usually thermal oxidation has been used to assure long time stability [8,20,21,22].

In biosensing applications of PS the biological analytes are attached to the pore walls hence the morphology (pore size and specific surface area (SSA)) plays an important role for the sensor sensitivity. In DBRs based on PSML the characteristic central line of the so-called stop-band shows a red shift which is inversely proportional to the average pore diameter [23]. According to these facts mesoporous silicon with small pore size and large SSA is preferred to achieve high sensor sensitivity [23]. Additionally, a red shift of the stop band occurs by loading the porous layers with appropriate biological solutions [23]. Thus, such PS multilayer structures have been introduced as key-component in optical biosensors [16].

The goal of the presented work is the detailed characterization of electrochemically etched porous silicon layers using heavily and lightly doped p-substrates, investigation of the influence of thermal oxidation on the material properties, realization and characterization of native and oxidized stacked structures using lightly doped p-substrate, functional testing using organic solvents and aqueous liquids and development of a cost-effective LED-based sensor measurement system.

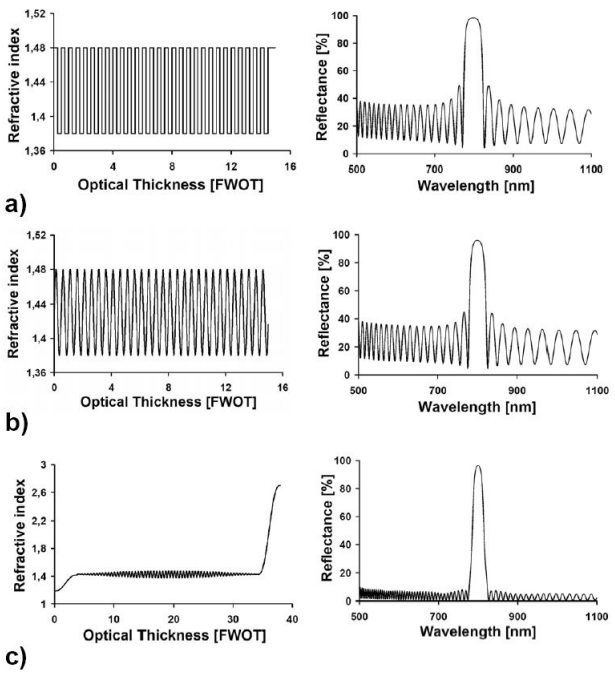

Figure 1. Simulated Multilayer structrures, left: depth profil of refractive index (FWOT:Full Wave Optical Thickness), right: corresponding simulated reflectance spectrum a) DBR with step-like refractive index change, b) Rugate with sinusoidal refractive index change, c) apodized and index matched rugate filter.

II. Optical Simulation of Porous Multilayers

Different multilayer structures have been simulated using Essential Macleod simulation software to analyze the optical properties and influences of the fabrication conditions, e.g. contrast of refractive index and layer number, on the reflectance spectra. Distributed Bragg Reflectors (DBRs) consist of a stack of two dielectric layers with step-like transition of high and low refractive index (n_h and n_l) and proper thicknesses (d_h and d_l), fulfilling the quarter-wave condition for the used light. In rugate filters the transition between high and low refractive indexes is varying continuously and periodically (e.g. sinusoidally). Apodization of the periodically variation of the index contrast eliminates the sidelobes while index matching to the boundary materials (in our case air and silicon substrate) suppresses ripples outside the stop band. Fig. 1 shows for different multilayer structures the depth profiles of the refractive index and the resulting simulated reflectance spectrum.

The stop band gap width of rugate filters is slightly smaller than that of a DBR filter. The sidelobes are effectively reduced using apodization. Further simulation results show that the width of the stop band is proportional to the amplitude of the refractive index modulation, while increasing the layer number increases reflectivity and sharpens the stop band gap.

III. Experimental

PS single layer structures have been formed by anodization of low doped (10-15Ωcm) and high doped (0.01-0.02Ωcm) (100)-oriented p-Si substrates. PS multilayer structures were formed only in low p-doped (10-15Ωcm) substrates. Anodization was performed in a solution of 30w.t.% aqueous HF(48%) with ethanol using a double-cell configuration. Under these conditions, the resulting porosity is very sensitive to current density variation, additionally a small pore size is obtained [18]. The formation rate of PS single layers was measured by Dektak150 after complete removal of the porous layer and the porosity (P) by a gravimetric technique. The anodization current was computer controlled by Konstanter 1500 PSP 60-60, so precise control of current densities, etch time and time dependence (e.g. step-like) was achieved. To obtain PSMLs the applied current density j was alternatively switched between 20 and 70mA/cm² for 20 and 3 seconds resulting in low and high porosity layers. A relaxation time of 1 second was applied after each layer formation (j= 0mA/cm²). PSMLs with 10 and 16 periods were designed to show a stop band gap peak of the DBR in the range of 700 and 750 nm (Fig. 5 and 6).

PSMLs were thermally oxidized by a two step process in pure oxygen (at 400°C for 1 hour and at 780°C for 30minutes) to change the hydrophobic surface property of as prepared porous silicon into hydrophilic. Temperatures were held low and oxidation times were held short to oxidize and activate the internal surface completely, but to avoid a complete pore filling by oxidation of the very small pores of the mesoporous material. The structural characterization of PSMLs was done using scanning electron microscopy (SEM).

N_2 adsorption/desorption isotherms were measured in Belsorp-mini of Co. Rubotherm/Bel at 77K and the pore size, pore size distribution and specific surface area (SSA) were evaluated using BET and BJH theory [25,26].

The PSMLs were characterized optically in a wide range of wavelengths (200-1100nm) with an Avaspec 2048-UA-50-AF spectrometer, using a halogen lamp source. The absolute reflectance was derived by referencing to reflection measurements on polished c-Si wafers.

IV. Results and Discussion

A. Properties of the PS single layers

Proper setting of the formation rate and the formation time allows to control and to design the thicknesses of layers with high and low refractive index. Fig. 2 shows for high and low doped p-substrates the measured porosity (left) and the corresponding refractive index values calculated using Bruggeman´s effective-medium-approximation [27] (right) given by equation (1):

$$P_{in}\frac{n_{air}^2-n_{eff}^2}{n_{air}^2+2n_{eff}^2}+(1-P_{in})\frac{n_{Si}^2-n_{eff}^2}{n_{Si}^2+2n_{eff}^2}=0 \qquad (1)$$

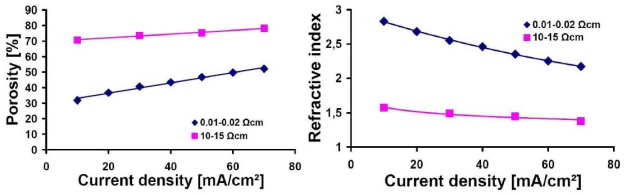

Figure 2. Porosity (left) and the corresponding refractive index calculated by Bruggeman`s model from equation (1) (right) of low ((10-15Ωcm) and high (0.01-0.02Ωcm) p-doped substrates in 30w.t.% aqueous HF(48%) with ethanol.

where P_{in} is the volume fraction of air in the porous material (i.e. porosity), n_{air}, n_{Si}, and n_{eff} are the refractive indices of air, silicon and effective porous medium, respectively.

As PSMLs are built up by very thin (typically some ten nm) layers, the relative small formation rate of PS in low doped p-substrates allows a better time control of the target thickness of an individual layer (typical formation time per layer: seconds). Formation rate R and porosity P are directly proportional to the current density j. The corresponding slopes $\Delta R/\Delta j$ and $\Delta P/\Delta j$ are slightly larger for highly doped p-Si than for low-doped p-Si. The dependence of the effective refraction index of PS on current density was calculated from P=f(j) using eq. (1) (Fig. 2, right). $\Delta n/\Delta j$ is larger for highly doped p-Si than for low-doped p-Si. Thus, the needed gradient of current density j to obtain layers with appropriate difference Δn for PSMLs is smaller for highly doped p-Si than for low-doped. However, the porosity is increasing with increasing current density for both, high and low p-doped material.

The dependence of current density on pore size and pore size distribution of as-fabricated PS (out of low doped p-Si) is shown in Fig. 3. By changing the anodization current density from 10mA/cm² to 30mA/cm² the mean pore size changes from 2.1nm to 2.6nm and the pore size distribution gets wider. However, it should be noted that these results were obtained at single layers (steady state conditions during anodization) whereas for very thin porous layers the according formation time is so small (typically seconds) that steady state situation is not reached.

PS layers formed from low doped p-substrates having small pore sizes in the range of 2-4 nm exhibit a large SSA of

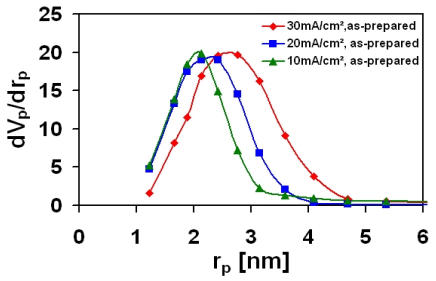

Figure 3. Pore size and its distribution of as- prepared PS layers using 10-30mA/cm² anodization and low-doped p-substrate.

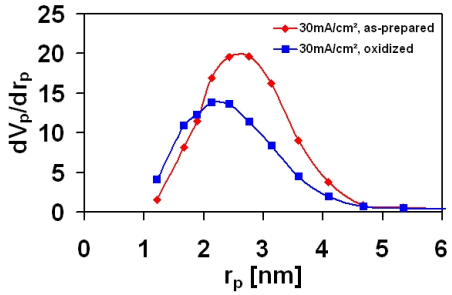

Figure 4. Pore size distribution of as- prepared and oxidized PS layers using p-susbstrate in 30w.t.% HF/Ethanol solution.

500-700m²/cm³, whereas for high doped p-substrates pore sizes are in the range of 3-12nm (p^+), 3-100nm (p^{++}) and the SSA is 170-230m²/cm³ depending on the PS formation conditions [18]. The morphology, mean pore size and SSA have to take into account for the design of PSMLs.

B. Properties of the thermally oxidized PS layers

Thermal oxidation of PS layer leads to stabilization of the internal surfaces and changes the hydrophobic surface properties into hydrophilic. Oxide formation causes expansion of the as-fabricated native porous network and results in pore size reduction. Fig. 4 shows one example of the pore size modification after a two-step oxidation as discussed in chap. III.

The oxidation rate in PS layers depends on the pore size and is considerably smaller than the surface oxidation rate especially for pore sizes in the low mesoporous range. The average pore size (peak value in distribution) is reduced by 0.5 nm and the porosity is reduced by 35% (from 75% to 40%) by the applied thermal oxidation. Therefore, a corresponding change of refractive index is expected including pore size reduction and material conversion (building of SiO_2). Similar reduction of porosity by oxidation was observed by J. Charrier et. al. [21] using heavily p-doped substrates. Very small pore size and porosity by thermal oxidation can especially occur in films formed at low current density because of the already lower initial porosity as demonstrated in Fig. 2 (left). Simultaneously the SSA of the PS layer after the oxidation step is reduced from 500-700m²/cm³ to 200-250m²/cm³.

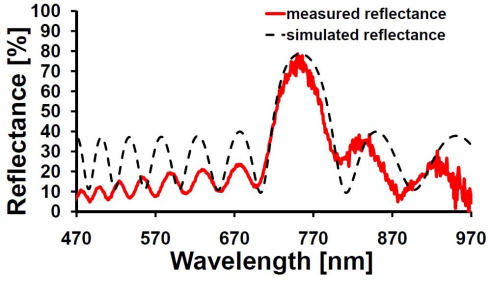

Figure 5. Measured and simulated reflectance of PS DBR using dH=127nm, dL=136nm and layer number=20 with pronounced resonant peak at 750nm.

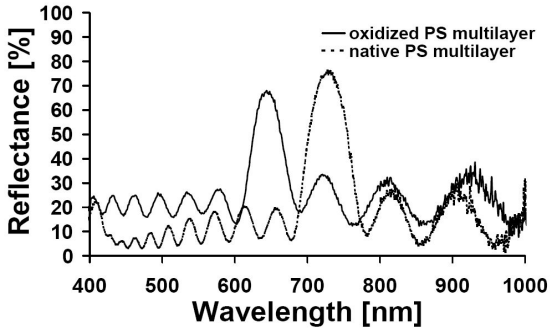

Figure 6. Reflectance of native and oxidized PS multilayers

C. Comparision of native and oxidized multilayers

DBR multilayers have been fabricated using low doped p-substrates to analyze the influence of the fabrication conditions on the spectral properties of PSML. Fig. 5 shows the measured and simulated reflectance of a DBR structure using as-fabricated PS with d_H=127nm, d_L=136nm and layer number=20. The measurement results can be well fitted with refractive indices of n_H=1.48 and n_L=1.38 and d_H=127nm, d_L=136nm in respect to spectral position and width of the stop band and sidelobes in the long wavelength range, however the measured sidelobes in the short wavelength range are quite smaller than simulated. This behavior has been reported also by other authors [7] and is referred to absorption and scattering phenomena which are not considered in simulation. The transition from low reflectance to high reflectance within the stop band is not very sharp and the bandwidth of the stop band is small. This is due to the small difference in refractive index of the two layers and the small number of layers.

The refractive indices of n_H=1.48 and n_L=1.38 obtained from the Macleod simulation correspond very well to the calculated refractive indices using Bruggeman´s theory (see Fig. 2 (right)).

Fig. 6 shows the influence of the thermal oxidation on the DBR reflectance. Oxidation causes a large blue shift of the peak position and a slight reduction of peak reflectivity. Additionally the stop band width is slightly reduced by oxidation which is related to the reduced difference in refractive index of the two layers after oxidation. This effect is more pronounced for longer oxidation times or higher oxidation temperatures as observed by Huanca et.al. [8].

D. Functional tests

Native and oxidized PSMLs were loaded by organic and aqueous analytes to prove the functionality of a sensor concept based on PSMLs. Methanol, ethanol and toluol were applied as analytes to sweep the refractive index. The refractive indices and the vapor pressures of the used solvents are summarized in Table 1.

Native oxide is hydrophobic for aqueous liquids. As a consequence the PSMLs layers with pore size in the lower mesoporous range are destroyed when filled with the aqueous solutions. Therefore, these layers are only suitable for the detection of organic solvents. Additionally, oxidized PSMLs exhibit hydrophilic surface property and in contrast to as-fabricated PSMLs were successfully used for both, organic solvents and aqueous analytes. Oxidized PSMLs provide a good reproducibility and long-time stability.

TABLE I. COMPARISION OF THE APPLIED ORGANIC SOLVENT PROPERTIES AND DESORPTION TIME MEASURED OPTICALLY IN NATIVE AND OXIDIZED PS

	Refractive index n	*Vapor pressure [hPa]*	*Measured desorption time in native PS [sec]*	*Measured desorption time in oxidized PS [min]*
Methanol	1.329	129	45	>20
Ethanol	1.36	58	63	>20
Toluol	1.496	29	180	>20

However, oxidation of the PSMLs reduces the spectral shift of the stop band peak ($\Delta\lambda$) for DBRs considerably as shown in Fig. 7. The spectral response to load by analytes is reduced for the oxidized samples due to the reduced porosity and the therefore smaller change of refractive index under load.

The wetting behavior of PS-layers can be characterized by contact angle measurements. The contact angles are in the range of 75°-105° for as-fabricated and of 20°-25° for oxidized PS layers [20]. Additionally, the time dependence of the spectral peak shift during evaporation of solvents out of the PSMLs by desorption provides information about the surface interactions between organic solvents and the porous material. In Table 1 typical desorption times of methanol, ethanol and toluol are summarized in native and oxidized DBRs. The time constants are measured from the time dependence of the peak shift $\Delta\lambda$ from its maximum value (saturation, pores filled maximally) back to its initial, unloaded value. The desorption time is decreasing with increasing vapor pressure of the different analytes and is essentially increased by oxidation of porous silicon which is another indication for stronger interaction between the liquids and the inner surfaces after oxidation. Furthermore, the desorption time depends on the temperature and humidity level, too.

Sugar solutions with various concentration were used as aqueous analytes for functional testing of the oxidized PSMLs. Peak shift from 35 to 55nm were measured for concentrations from 1w.t% to 50w.t.% which corresponds to a change of the effective refractive index from 1.334 to 1.42. The oxidized samples show a high mechanical stability and reproducibility even after multiple wetting and drying processes.

E. Optical measurement system

With PSMLs it is possible to realize simply by appropriate anodization times and sequences a variety of basic optical structures such as DBR, Fabry-Perot or Rugate filters (Fig.1). Using an optimized optical structure for the provided change

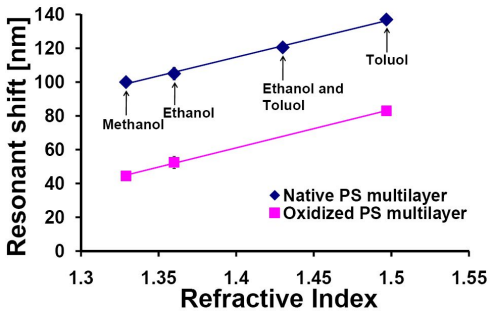

Figure 7. Spectral shift of stop band peak for native and oxidized PSMLs as the function of the refractive index of the used organic analytes.

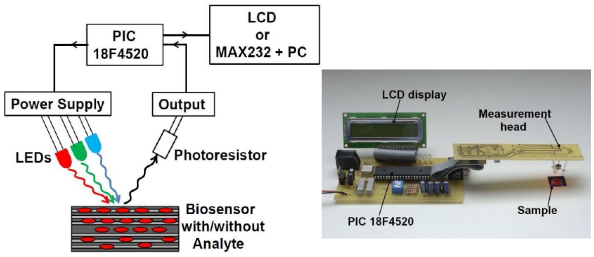

Figure 8. Schematic set-up of the developed optical sensor system (left) and the realized circuit with the main units and schematically sample position under the measurement head without housing.

of refractive index in the PSML for a given analyte, low cost optical components can be used to read-out the according spectral information. A first prototype is sketched in Fig. 8. The optical measurement setup consists of lamp source, light guides, light detector and additional signal processing units. Instead of a conventional spectrum analyzer which is expensive and hard to miniaturize a cost-effective and transportable evaluation system was developed. In the proposed system the light sources are three different LEDs (red, green and blue). The total reflection is detected by a photoresistor. The measurement results are displayed on a LCD panel. With serial port communication it is possible to connect the device to a computer and to perform time depending reflectance measurements. Fig. 8 shows the schematic setup of a simple optical evaluation system (left) and the realized prototype with the main units such as signal evaluation unit and measurement head (right). The implementation of the developed system and determination of the suitable application areas with the corresponding resolutions is actually in evaluation.

V. CONCLUSION

Optical simulation has been successfully used to optimize the optical behavior of different PSMLs. Electrochemically etched PS single layers have been fabricated and characterized using heavily and lightly doped p-substrates. PS layers realized in lightly doped p-substrates exhibit high porosity from 70% to 80% and pore size in the range of 2-4nm. Additional oxidation causes material conversion from Si to SiO_2 and a corresponding pore size reduction of 0.5nm with an essential reduction of porosity (approximately 35%) which results in a change of the effective refractive indices of the two layers forming the PSMLs.

DBR stacks were realized and investigated to analyze the influence of the fabrication conditions on the reflectance spectra. Oxidation produces blue-shift in the reflectance spectra and a small reduction of the peak reflectivity.

Both, native and oxidized DBRs using lightly p-doped substrates provide large spectral shifts of stop band peak for organic solvents. Native PS layers shows hydrophobic surface properties and are not suitable for detection of aqueous solutions due to low mechanical stability of the PSML-structures. In contrast, oxidized stacks can be used for both, for organic solvents and aqueous solutions and provide a good reproducibility and long-time stability.

The developed LED-based sensor system provides a low cost and miniaturized in-situ measurement possibility for different organic and aqueous solutions.

ACKNOWLEDGMENT

The authors would like to thank for the financial support of the Landesstiftung Baden-Wuerttemberg and the EU (EFRE) for the project “Photonic Methods in New Dimensions-Photon^{n}”.

REFERENCES

[1] S. Chan, P. M. Fauchet, Y.Li, L.J.Rothberg and B.L.Miller, “Porous silicon microcavities for biosensing applications”, Phys. Stat. Sol. A, vol. 182, p. 541-546, 2000.

[2] A. Jane, R. Dronov, A. Hodges and N.H. Voelcker, “Porous silicon biosensors on the advance”, Trends in Biotechnology, Vol 27 No.4, pp.230-9, Feb 27 2009

[3] E. J. Anglin, L. Cheng, W. R. Freeman and M.J. Sailor, “Porous silicon in drug delivery devices and materials”, Advanced Drug Delivery Reviews, 60, pp.1266-1277, 2008

[4] S. M. Weiss, G. Rong and J.L. Lawrie, “Current status and outlook for silicon-based optical sensors”, Phy. Stat. Sol., A 206,pp-1365-1368, 2009.

[5] G. Palestino, R. Legros, V. Agarwal, E. Pérez and Cs. Gergely, “Funtionalization of nanostructured porous silicon microcavities for glucose oxidase detection”, Sensors and Actuators, B135, pp. 27-34, 2008.

[6] F. Cunin, T. A. Schmedake, J. R. Link, Y. Li, J. Koh, S. Bathia and M. Sailor, “Biomolecular screening with encoded porous-silicon photonic crystals”, Nature mater 1, pp.39-41, 2002

[7] M.S. Salem, M.J. Sailor, K. Fukami, T. Sakka and Y. H. Ogata, “Sensitivity of porous silicon rugate filters for chemical vapor detection”, J. Appl. Phys. 103, 083516-1-7, 2008.

[8] D. R. Huanca, F. J. Ramirez-Fernandez and W. J. Salcedo, “Porous silicon optical cavity structure applied to high sensitivity organic solvent sensor”, Microelectronic Journal 39, pp. 499-506, 2008

[9] M. G. Berger, R. Arens-Fischer, M. Thönissen, M. Krüger, S. Billat, H. Lüth, S. Hilbrich, W. Theiss amd G. Grosse, “Dielectric filters made of PS: advanced performance by oxidation and new layer structures”, Thin Solid Films 297, pp. 237-240, 1997

[10] E. Lorenzo, C. J. Oton, N. E. Capuj, M. Ghulinyan, D. Navarro-Urrios, Z. Gaburro, L. Pavesi, “Porous silicon-based rugate filter”, Applied Optics, Vol. 44, No. 26, pp. 5415-5421, 2005

[11] M. S. Salem, M. J. Sailor, T. Sakk, Y. H. Ogota, " Electrochemical preparation of a rugate filter in silicon and ist deviation from the ideal structure", J. of Appl. Phys. 101, pp. 063503-1-6, 2007

[12] N. Ishikura, M. Fujii, K. Nishida, S. Hayashi, J. Diener, M. Mizuhata and S. Deki, "Broadband rugate filters based on porous silicon, Optical Materials 31, pp. 102-105, 2008

[13] S. Ilyas, T. Böcking, K. Kilian, P. J. Reece, J. Gooding, K. Gaus and M. Gal, " Porous silicon based narrow line-width rugate filter", Optical Materials 29, pp. 619-622, 2007

[14] V. S.-Y. Lin, K. Motesharei, K.-P. S. Dancil, M.J. Sailor, M. R. Ghadiri, "A Porous Silicon-Based Optical Interferometric Biosensor", Science, vol. 278, pp.840-843, 1997

[15] J. Chapron, S. A. Alekseev, V. Lysenko, V.N. Zaitsev, D. Barbier, "Analysis of interaction between chemical agents and porous Si nanostructures using optical sensing properties of infra-red Rugate filters", Sensors and &Actuators, B 120, p. 706-711, 2007.

[16] V. Torres, F. Agulló-Rueda, R.J. Martin-Palma, J. M. Martinez-Duart, "Porous silicon optical devices for sensing applications", Optical materials 27, pp. 1084-1087, 2005.

[17] M. Ghulinyan, C. J. Oton, G. Bonetti, Z. Gaburro and L. Pavesi,"Free-standing porous silicon single and multiple optical cavities",J. of Appl. Phys., vol. 93, nr. 12, pp. 9724-9729, 2003

[18] L. Canham, "Properties of Porous Silicon", INSPEC, ISBN 0852969325, 1997

[19] L. Pavesi and V. Mulloni, "All porous silicon microcavities: growth and physics", J. of Luminescensce 80, pp.43-52, 1999

[20] A. Kovacs, D. Meister, U. Mescheder, "Investigation of humidity adsorption in porous silicon layers"., Phys. Stat. Sol. A 206, No.6, pp.1343-1347, 2009

[21] J. Charrier , V. Alaiwan, P. Pirasteh, A. Najar and M. Gadonna, "Influence of experimantal parameters on physical properties of porous silicon and oxidized porous silicon layers", Applied Surface Science 253, pp. 8632-8636, 2007

[22] M.S. Salem, M.J. Sailor, F.A. Harraz, Y.H. Ogota, "Electrochemical stabilization of porous silicon multilayers for sensing various chamical compounds", J. of Appl. Phys. 100, pp. 083520-1-7, 2006

[23] H. Ouyang and P. M. Fauchet, "Biosensing using Porous Silicon Photonic Bandgap Structures, Photonic crystals and Photonic Crystal fibers for sensing applications, in Photonic crystas and Photonic crystal fibersfor Sensing Applications,Proceedings of SPIE, pp.600508 1-15, 2005

[24] J. Volk, J. Balázs, A.L. Tóth, I. Bársony, "Porous silicon multilayers for sensing by tunable IR-transmission filtering", Sensors and Actuators B100, pp. 163-167, 2004

[25] E.P. Barrett, L.G. Joyner and P.H. Halenda, "The Determination of Pore Volume and Area Distribution in Porous Substances. I. Computations from Nitrogen Isotherms", J. Am. Chem. Soc. 73, pp.373-380, 1951

[26] S. Brunauer, P. H. Emmett and E. Teller, "Adsorption of Gases in Multimolecular Layers", *J. Am. Chem. Soc.*, 60, pp.309-319, 1938

[27] W. Theiss, in Festkörperprobleme/Advances in Solid State Physics, edited by R. Helbing (Vieweg, Braunschweig), Vol. 33, pp. 149, 1994